Kinetic Isotope Effects for Cl + CH 4 ⇌ HCl + CH 3 Calculated Using ab Initio Semiclassical Transition State Theory

ARTICLE *in* THE JOURNAL OF PHYSICAL CHEMISTRY A · FEBRUARY 2012

Impact Factor: 2.69 · DOI: 10.1021/jp212383u · Source: PubMed

3 AUTHORS:

John R. Barker
University of Michigan
171 PUBLICATIONS **5,945** CITATIONS
SEE PROFILE

Thanh Lam Nguyen
University of Texas at Austin
72 PUBLICATIONS **1,382** CITATIONS
SEE PROFILE

John F Stanton
University of Texas at Austin
5 PUBLICATIONS **75** CITATIONS
SEE PROFILE

THE JOURNAL OF PHYSICAL CHEMISTRY A

Article

pubs.acs.org/JPCA

Kinetic Isotope Effects for Cl + CH_4 ⇌ HCl + CH_3 Calculated Using ab Initio Semiclassical Transition State Theory

John R. Barker,*[,†] Thanh Lam Nguyen,[†,§] and John F. Stanton*[,‡]

[†]Department of Atmospheric, Oceanic and Space Sciences, University of Michigan, Ann Arbor, Michigan 48109-2143, United States

[‡]Department of Chemistry and Biochemistry, The University of Texas, Austin, Texas 78712-0165, United States

Supporting Information

ABSTRACT: Calculations were carried out for 25 isotopologues of the title reaction for various combinations of ^{35}Cl, ^{37}Cl, ^{12}C, ^{13}C, ^{14}C, H, and D. The computed rate constants are based on harmonic vibrational frequencies calculated at the CCSD(T)/aug-cc-pVTZ level of theory and X_{ij} vibrational anharmonicity coefficients calculated at the CCSD(T) /aug-cc-pVDZ level of theory. For some reactions, anharmonicity coefficients were also computed at the CCSD(T)/aug-cc-pVTZ level of theory. The classical reaction barrier was taken from Eskola et al. [*J. Phys. Chem. A* **2008**, *112*, 7391−7401], who extrapolated CCSD(T) calculations to the complete basis set limit. Rate constants were calculated for temperatures from ∼100 to ∼2000 K. The computed ab initio rate constant for the normal isotopologue is in good agreement with experiments over the entire temperature range (∼10% lower than the recommended experimental value at 298 K). The ab initio H/D kinetic isotope effects (KIEs) for CH_3D, CH_2D_2, CHD_3, and CD_4 are in very good agreement with literature experimental data. The ab initio $^{12}C/^{13}C$ KIE is in error by ∼2% at 298 K for calculations using X_{ij} coefficients computed with the aug-cc-pVDZ basis set, but the error is reduced to ∼1% when X_{ij} coefficients computed with the larger aug-cc-pVTZ basis set are used. Systematic improvements appear to be possible. The present SCTST results are found to be more accurate than those from other theoretical calculations. Overall, this is a very promising method for computing ab initio kinetic isotope effects.

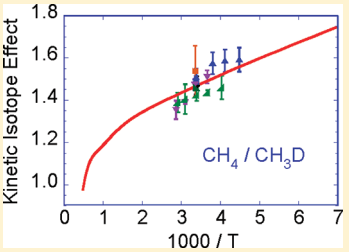

INTRODUCTION

Methane is a natural, biogenic constituent of the atmosphere. Its atmospheric lifetime of ∼12 years is controlled mostly by its reaction with hydroxyl radicals and secondarily by its reactions with chlorine atoms and $O(^1D)$.[1] Laboratory data for reaction rates can be used with estimated concentrations of the reactive radicals to ascertain the relative importance of these atmospheric "sink" reactions. The gas phase reaction of chlorine atoms with methane is the second-most important sink reaction (after reaction with OH) for methane. The reaction (and its reverse) has been the subject of many experimental[2,3] and theoretical studies. A more direct source of knowledge about the atmospheric sinks in comparison to each other and to other physical processes, like transport and mixing, can be obtained from the isotopic composition of atmospheric methane.[4−8]

The primary sources of atmospheric methane have distinct isotopic signatures, which are affected by fractionation in the atmosphere. Isotopic fractionation, described by the Rayleigh fractionation equation,[9−11] occurs because different isotopologues react at different rates. The isotopologue that reacts most quickly is depleted and the one that reacts most slowly is enriched in the atmosphere. The reaction of the isotopologue is characterized by a distinct kinetic isotope effect (KIE), or fractionation factor α, which is defined as a ratio of rate constants:

$$\alpha = \frac{k(\text{light})}{k(\text{heavy})} \quad (1)$$

where by convention the rate constant involving the lighter isotopologue appears in the numerator.

The Arrhenius plot of the rate constant for the title reaction is distinctly curved (Figure 1), which suggests that quantum mechanical tunneling is important. Quantum mechanical tunneling is one of the causes of "mass-independent" isotope effects, which are of considerable atmospheric interest.[12] Because of its importance and because of the extensive experimental rate constant data available for comparisons,[2,3] this reaction provides a useful test for semiclassical transition state theory (SCTST).

SCTST was developed by Miller and colleagues.[13−16] We recently developed a new implementation, which can be applied to reactions involving up to a dozen or so atoms.[17] As a test, we applied SCTST to the reaction OH + H_2 and its H/D isotopologues.[18] That reaction included a small enough number of electrons so that very high levels of theory could be used to

Special Issue: A. R. Ravishankara Festschrift

Received: December 22, 2011
Revised: January 31, 2012

   dx.doi.org/10.1021/jp212383u | *J. Phys. Chem. A* XXXX, XXX, XXX−XXX

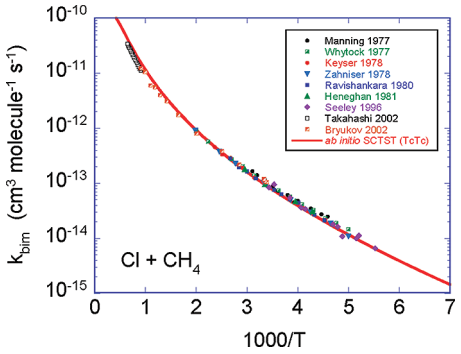

Figure 1. Absolute thermal rate constant for Cl + CH_4. Experimental measurements are shown by the symbols. The absolute rate constant was obtained for ^{35}Cl + $^{12}CH_4$ by using the TcTc data set and the DBOC computed at the CCSD/aVTZ level of theory.

calculate highly accurate thermochemistry. The CFOUR electronic structure code[19] was modified to utilize its analytical first and second derivatives for coupled cluster theory with single and double excitations, with a perturbative treatment of triple excitations (CCSD(T)), for computing the vibrational anharmonicies (X_{ij}) of transition states. The calculated results agreed essentially perfectly with the experimental data. SCTST promises to be highly accurate because it intrinsically includes zero point energy, multidimensional quantum tunneling along the curved reaction path, and anharmonicity and nonseparable coupling among all vibrational degrees of freedom, including the reaction coordinate. In conventional transition state theory, which is based on classical mechanics, all of these nonclassical features are either neglected or added ad hoc. SCTST does not require such empiricisms.

However, further testing is needed to clearly understand the strengths and limitations of the theory and how it is implemented. SCTST is based on second-order vibrational perturbation theory (VPT2),[20] which neglects higher-order terms that may be important in some cases. Although not required by the theory, we have treated vibration and rotation as separable in our current implementation. For the OH + H_2 reaction, neither of these potential limitations was significant.

The Cl + CH_4 reaction provides a demanding test for SCTST and its implementation. The reaction transition state contains of 12 vibrational degrees of freedom and includes 27 electrons, compared with 6 and 11, respectively for the OH + H_2 reaction. For the OH + H_2 reaction, HEAT-345Q theory[21−23] was feasible for accurately computing the thermochemistry. For Cl + CH_4, that level of theory is prohibitively expensive. However, Eskola et al.[24] used the CCSD(T) level of theory, extrapolated to the complete basis set limit (CBS), to compute the reaction thermochemistry, with expected errors of $\lesssim$4 kJ/mol. The present work shows that the errors are probably much smaller than that for this particular system, however. Moreover, the calculated KIEs are not sensitive to small errors in the classical barrier height and therefore the ab initio rate constants could be used without adjustments to obtain the ab initio KIEs reported here.

In the following sections, the quantum chemistry and chemical kinetics methods are described, followed by a description of the results and discussion in the context of previous work. In the final section of the paper, our conclusions are briefly summarized.

METHODS

Ab Initio Calculations. Previously, Eskola et al. reported optimized geometries of various species including CH_4, CH_3, HCl, and the transition structure (TS) for the title reaction, which they obtained at the QCISD/6-311G(d,p) level of theory.[24] They then used the optimized geometries with coupled-cluster theory involving single, double, and a perturbative treatment of triple excitations (CCSD(T)),[25] to compute the reaction barrier and thermochemistry. They extrapolated results obtained with the aug-cc-pVDZ, aug-cc-pVTZ, and aug-cc-pVQZ Dunning correlation consistent basis sets to the complete basis set (CBS) limit to obtain the classical reaction barriers in the forward and reverse directions for the title reaction: 32.11 and 7.80 kJ/mol, respectively, including the electronic spin splitting correction[26] of 3.51 kJ/mol for the Cl atom.

In the present work, SCTST is used for computing thermal (canonical) rate constants. As described in detail elsewhere (and summarized below), SCTST requires harmonic vibrational frequencies and anharmonicity coefficients (X_{ij}). To obtain these quantities, the geometries at stationary points on the PES were reoptimized at the CCSD(T)/aug-cc-pVTZ (hereafter designated as aVTZ) level of theory using extremely tight optimization convergence thresholds. All core electrons were kept frozen. In calculations carried out with the CFOUR program,[19] harmonic vibrational frequencies were determined using the analytical gradients available in the code. Twenty-five distinct isotopic reactions (involving combinations of ^{35}Cl, ^{37}Cl, ^{12}C, ^{13}C, ^{14}C, H, and D) were considered in this work (see Supporting Information). The aVTZ basis set was chosen because our unpublished calculations on OH + H_2 and OH + CO suggested that imaginary frequencies converge to the CBS limit more rapidly with augmented basis sets than with others, as the ordinal number of the basis set is increased.[27]

Second-order vibrational perturbation theory (VPT2), which is implemented in a special version of CFOUR, was used to obtain the X_{ij} anharmonicity coefficients both for the stable molecular species and for the transition structure. The full cubic force field and the semidiagonal part of the quartic force field were obtained by differentiating the harmonic force constants numerically with respect to the molecular normal coordinates. In all cases where harmonic frequencies are within 100 cm^{-1} of zeroth-order level positions corresponding to two quantum transitions (signifying potential Fermi resonances) standard deperturbation techniques were applied. Moreover, the computations are computationally expensive.

To save expense, most anharmonicities were computed using the smaller aug-cc-pVDZ basis set (hereafter designated as aVDZ), but some were obtained with the aVTZ basis. When combined with harmonic vibrational frequencies obtained with the aVTZ basis, this leads to two combinations of vibrational data generated by CFOUR, designated TcTc and TcDc (where T and D denote the aVTZ and aVDZ basis sets, respectively, and the "c" designates CFOUR). The latter set, a hybrid, is analogous to the hybrid used to obtain accurate results by Lee, Martin and Taylor (LMT) in a study of anharmonic force fields of CH_4 isotopologues.[28]

In a separate series of calculations, the GAUSSIAN program[29] was also used for geometry optimizations and for computing harmonic vibrational frequencies at the CCSD(T)/aVTZ level of theory. Because the Gaussian program lacks analytical gradients for the CCSD(T) method, the eigenvalue-

dx.doi.org/10.1021/jp212383u | J. Phys. Chem. A XXXX, XXX, XXX−XXX

following algorithm was used for optimization with the extremely tight optimization convergence criterion (i.e., Opt=(EF,VeryTight)). All core electrons were frozen. The initial guess for the optimization step was taken from the optimized geometry and Hessian obtained at the MP2(full)/6-31+G(d,p) level of theory. Harmonic vibrational frequencies were then determined by double numerical differentiation of the CCSD(T) energies (i.e., Freq=EnOnly).

The harmonic frequencies computed using GAUSSIAN were combined with the anharmonicities computed with CFOUR using the aVDZ basis set to define a third set of vibrational parameters designated TgDc. The small differences between the TcDc and TgDc data sets are only due to round off errors and differences in numerical differentiation procedures, and the resulting rate constants are essentially identical. Thus the TgDc and TcDc data sets were used interchangeably. In all rate constant calculations labeled "TgDc" (or "TcTc"), the vibrational and rotational parameters for the reactant species (i.e., methane, methyl radicals, and hydrochloric acid) were taken from the TcDc (or TcTc) data sets, whereas those for the transition states were taken from the TgDc (or TcTc) data sets.

The CCSD(T) method is based on the Born−Oppenheimer approximation, which generates mass-independent PESs. Mass-dependent PESs, which are more accurate, are obtained by applying the diagonal Born−Oppenheimer correction (DBOC) obtained using perturbation theory. The DBOC for all isotopic species was obtained using the HF/aVTZ level of theory. In addition, the CCSD/aVTZ level of theory was used to obtain the DBOC for all of the species involved in two reactions: $^{35}Cl + {}^{12}CH_4$ and $^{35}Cl + {}^{13}CH_4$. All of the DBOC calculations were carried out for optimized geometries obtained at the CCSD-(T)/aVTZ level of theory. For reaction barriers, the differences in DBOCs obtained by the HF method are less than 35 cm^{-1} and those obtained using the CCSD level of theory are less than 25 cm^{-1}. These DBOC energy differences are small, compared with possible errors of 2−3 kJ mol^{-1} in the computed barrier heights, but they are significant for the H/D KIEs at low temperatures. For $^{12}C/^{13}C$ KIEs, the DBOC is essentially insignificant (<0.3 cm^{-1}).

As discussed by Eskola et al.,[24] a hydrogen-bonded adduct exists between CH_3 and HCl. Its energy (including zero point energy, ZPE) is lower than the energy of Cl + CH_4, i.e., an exothermic reaction. If the adduct is ignored, the reaction is endothermic. Because formation of the adduct is exothermic, it is possible for the system to tunnel through the energy barrier in the forward direction to produce the adduct. It is also possible for CH_3 and HCl to form the adduct, when the reaction proceeds in the reverse direction, if collisional stabilization is significant. However, the chance of collisional stabilization is very small, because the adduct is weakly bound and its lifetime is expected to be much shorter than typical average time intervals between collisions, even at pressures substantially greater than 1 bar.

To test for the possible effects of the adduct on the computed rate constant in the forward direction, SCTST calculations were carried out for both the exothermic (i.e., explicitly including the adduct) and endothermic (i.e., ignoring the adduct) models. The rate constants computed for these two models were found to be differ by <0.1% at temperatures above 140 K. Thus the endothermic model was used in all subsequent calculations.

Rate Constant Calculations. *Semi-Classical Transition State Theory.* SCTST was developed by Miller and co-workers and has been described thoroughly elsewhere.[13,14,16−18,30] The canonical rate constant, $k(T)$, can be expressed as the thermal average of a microcanonical rate constant, $k(E)$:

$$k(T) = \frac{1}{h}\frac{\int_{-\infty}^{\infty} G^{\ddagger}(E)\exp(-E/k_BT)\,dE}{Q_{re}(T)} \tag{2a}$$

where h is Planck's constant, k_B is Boltzmann's constant, T is the temperature, $\rho(E)$ is the density of states of the reactant, Q_{re} is the total partition function of the reactant(s), and $G^{\ddagger}(E)$ is the cumulative reaction probability (CRP).[30]

$$k(E) = \frac{1}{h}\frac{G^{\ddagger}(E)}{\rho(E)} \tag{3}$$

At moderate temperatures, couplings between rotations and vibrations can be neglected, giving

$$k(T) = \frac{1}{h}\frac{Q_t^{\ddagger}Q_r^{\ddagger}}{Q_tQ_r}\frac{\int_{-\infty}^{\infty} G_v^{\ddagger}(E_v)\exp(-E_v/k_BT)\,dE_v}{Q_v(T)} \tag{2b}$$

in which vibrational energy E_v is the variable of integration. The corresponding CRP is given by

$$G_v^{\ddagger}(E_v) = \sum_{n_1}\sum_{n_2}\cdots\sum_{n_{F-2}}\sum_{n_{F-1}} P_n(E_v) \tag{4}$$

where the semiclassical tunneling probability P_n is[14]

$$P_n(E) = \frac{1}{1+\exp[2\theta(n,E)]} \tag{5}$$

The barrier penetration integral $\theta(n,E)$ and related quantities are given by

$$\theta(n,E) = \frac{\pi\Delta E}{\Omega_F}\frac{2}{1+\sqrt{1+4x_{FF}\Delta E/{\Omega_F}^2}} \tag{6}$$

$$\Delta E = \Delta V_0 + G_0 - E + \sum_{k=1}^{F-1}\omega_k\left(n_k+\frac{1}{2}\right) + \sum_{k=1}^{F-1}\sum_{l=k}^{F-1}x_{kl}\left(n_k+\frac{1}{2}\right)\left(n_l+\frac{1}{2}\right) \tag{7}$$

$$\Omega_F = \bar{\omega}_F - \sum_{k=1}^{F-1}\bar{x}_{kF}\left(n_k+\frac{1}{2}\right) \quad \text{with} \quad \bar{\omega}_F = -i\omega_F \quad \text{and} \quad \bar{x}_{kF} = ix_{kF} \tag{8}$$

In these expressions, F is the number of internal degrees of freedom of the transition state, ordered so that the reaction coordinate is last (i.e., has index F); ω_k is the harmonic vibrational frequency of the kth vibration, ω_F is the imaginary frequency associated with the reaction coordinate, x_{kl} are the vibrational anharmonicity constants for the degrees of freedom orthogonal to the reaction coordinate, x_{kF} are the (pure imaginary) coupling terms between the reaction coordinate and the orthogonal degrees of freedom, x_{FF} is the (pure real) anharmonicity constant for the reaction path, and ΔV_0 is the classical barrier height. The term G_0 is a constant, which is irrelevant in spectroscopic measurements (where only energy differences are important), but which must be included for

dx.doi.org/10.1021/jp212383u | J. Phys. Chem. A XXXX, XXX, XXX−XXX

thermochemistry and kinetics.[31] Terms labeled as anharmonic zero point energies always include G_0.

The algorithm described by Nguyen et al.[17,18] was used to compute the CRP. The algorithm is based on the algorithms of Wang and Landau[32] and Basire et al.,[33] as extended by Nguyen and Barker.[34] The Nguyen−Barker algorithm[34] was used for computing the partition functions for the fully coupled anharmonic vibrations of methane. Computer programs SCTST and ADENSUM for computing the CRP and the partition function for the anharmonic coupled vibrations in methane, respectively, were used in conjunction with program THERMO to compute the thermal rate constants; all three codes are included in the MULTIWELL Program Suite.[35,36] Computing microcanonical rate constants and then taking the thermal average is not the most efficient approach for obtaining canonical rate constants, but this capability is essential for master equation calculations. Efficient methods for directly computing SCTST thermal rate constants exist[16] but were not used in the present work.

The DBOC was applied after computing SCTST rate constants on the Born−Oppenheimer potential energy surface. It was applied as described by Mielke et al.,[37] as shown:

$$k(\text{corrected}) = k\mathrm{e}^{-\Delta_{\mathrm{DBOC}}/k_{\mathrm{B}}T} \tag{9}$$

where

$$\Delta_{\mathrm{DBOC}} = (\mathrm{DBOC})_{\text{transition state}} - \sum_{i}^{\text{reactants}} (\mathrm{DBOC})_i \tag{10}$$

Reactions. The reaction types considered in the present work are listed in Table 1. For most of the reactions, harmonic frequencies and vibrational anharmonicities were computed separately for reactions involving ^{35}Cl and ^{37}Cl, but in some cases only ^{35}Cl was considered. The computed rate constants for the two chlorine isotopes were combined by weighting them according to their natural abundance[38] (f_{35} = 0.7576, f_{37} = 0.2424). Reaction rates involving H, D, ^{13}C, and ^{14}C were computed. Because of the large number of isotopic combinations, the reaction numbering is according to the code given in Table 1. The code distinguishes between abstraction of H and D atoms, such as in the reaction Cl + CH_3D. In this reaction, as in the others when two reaction channels exist, the total rate constant is assumed to be the sum of the rate constants computed for the individual channels.

Table 1. Reactions

number[a]	forward reactions
*nm*hch3	Cl + CH_4 → HCl + CH_3
*nm*hch2d	Cl + CH_3D → HCl + CH_2D
*nm*dch3	Cl + CH_3D → DCl + CH_3
*nm*hchd2	Cl + CH_2D_2 → HCl + CHD_2
*nm*dch2d	Cl + CH_2D_2 → DCl + CH_2D
*nm*hcd3	Cl + CHD_3 → HCl + CD_3
*nm*dchd2	Cl + CHD_3 → DCl + CHD_2
*nm*dcd3	Cl + CD_4 → DCl + CD_3
number[a]	reverse reactions
−*n*2hch3	HCl + CH_3 → Cl + CH_4
−*n*2dch3	DCl + CH_3 → Cl + CH_3D
−*n*2hcd3	HCl + CD_3 → Cl + CHD_3
−*n*2dcd3	DCl + CD_3 → Cl + CD_4

[a]Integers *n* and *m* denote chlorine and carbon isotopes, respectively. ^{35}Cl and ^{37}Cl are denoted by *n* = 5 and 7, respectively. ^{12}C, ^{13}C, and ^{14}C are denoted by *m* = 2, 3, and 4, respectively. The first symbol following *m* denotes the atom transferred from methane to chlorine. For example, the reaction number 72dch2d corresponds to abstraction of a D-atom in the reaction ^{37}Cl + $^{12}CH_2D_2$ → D^{37}Cl + $^{12}CH_2D$. When *n* is omitted, the rate constant refers to the natural abundance of the Cl isotopes; when *m* is omitted, the rate constant refers to ^{12}C.

The partition function for anharmonic vibrations computed by ADENSUM is based on the standard form:

$$q_{\mathrm{vib}} = \int_0^{E_{\max}} \rho(E)\mathrm{e}^{-E/k_{\mathrm{B}}T}\,\mathrm{d}E \tag{11}$$

where E is the vibrational energy above the zero point energy, $\rho(E)$ is the density of states, and $E_{\max}$ is ideally equal to infinity, but for computational purposes is set to a large but finite energy. In all calculations, the energy grain size used for computing the numerical density of states[34] was set to 5 cm^{-1}, which is $\ll k_{\mathrm{B}}T$, even at low temperatures. The maximum energy, $E_{\max}$ was set to 20 000 cm^{-1}, which is sufficiently high so that it does not significantly truncate the thermal population distribution at $T \leq 2000$ K. We estimate that the rate constant at 2000 K is reduced by <5% due to this truncation error.

RESULTS AND DISCUSSION

Ab initio Calculations. Optimized geometries, harmonic vibrational frequencies, rotational constants, and anharmonicities are summarized in the Supporting Information. The energies obtained for the optimized structures using CFOUR and GAUSSIAN-09 differ by less than 0.02 cm^{-1} and the geometries differ by only 0.0007 Å in the C−H bond, 0.0003 Å in the Cl−H bond, and 0.01° in the HCH angle. These small differences are due to the different optimization convergence criteria implemented in the two programs. The harmonic zero point energies (ZPE_h) obtained using the two programs differ by <3 cm^{-1}, as shown in Table 2. These small differences have a negligible effect on the computed rate constants and could be used interchangeably.

Table 2. Vibrational Data Sets[a] for the ^{35}Cl−H−$^{12}CH_3$ Transition State

data set[b]	ZPE_h	$0.25\sum X_{ij}$	G_0	ZPE_{anh}
TcTc	8369.8	−67.4	−134.2	8168.2
TgDc	8371.8	−38.3	−144.1	8189.4
TcDc	8369.8	−38.3	−144.1	8187.4

[a]Energies expressed in units of cm^{-1}. [b]Harmonic vibrational frequencies and anharmonicities constitute a data set. D and T denote aVDZ and aVTZ basis sets, respectively; c and g denote CFOUR and GAUSSIAN computer codes, respectively. The first and second terms describe the details for computing the harmonic frequencies and vibrational anharmonicities, respectively.

The implementation of VPT2 in CFOUR produces anharmonicities for symmetries corresponding to asymmetric tops. For symmetric tops the calculations are carried out in reduced symmetry and the anharmonicities are expressed in the reduced symmetry. For example, the symmetry of CH_4 is reduced from T_d to C_{2v} that for CH_3D is reduced from C_{3v} to C_s for the purpose of computing the anharmonicities. Because the anharmonicities are expressed in the lower symmetry, they cannot be readily compared to literature values. However, for CH_2D_2, which has C_{2v} symmetry, the anharmonicities are

dx.doi.org/10.1021/jp212383u | J. Phys. Chem. A XXXX, XXX, XXX−XXX

Table 3. Harmonic and Fundamental Frequencies for CH_2D_2

		harmonic frequency (cm^{-1})			fundamental frequency (cm^{-1})			
index	sym	this work[a]	LMT[c]	exptl[d]	this work[a]	this work[b]	LMT[c]	exptl[d]
1	A1	3092.8	3102.5	3104.4217	2949.9	2962.9	2972.1	2971.605
2	A1	2230.0	2236.9	2237.9855	2154.0	2161.4	2167.7	2175.683
3	A1	1474.8	1470.9	1472.3115	1441.1	1435.7	1435.7	1434.842
4	A1	1056.8	1053.1	1054.4405	1038.1	1035.0	1033.9	1032.176
5	A2	1363.0	1360.1	1361.2375	1335.6	1330.7	1330.7	1331.490
6	B1	3145.9	3156.5	3159.7912	2987.4	2997.9	3008.0	3012.031
7	B1	1120.6	1116.2	1117.7847	1097.5	1093.8	1093.5	1088.159
8	B2	2328.9	2337.1	2339.5713	2237.9	2242.1	2246.6	2254.608
9	B2	1270.9	1265.7	1267.4576	1243.7	1238.8	1235.3	1236.874

[a]Present work: harmonic frequencies and anharmonicity constants were obtained using the CCSD(T)/aVTZ and CCSD(T)/aVDZ levels of theory, respectively. [b]Present work: both the harmonic frequencies and the anharmonicity constants were calculated using the CCSD(T)/aVTZ level of theory. [c]Reference 28: obtained from CCSD(T)/cc-pVTZ cubic and quartic force field combined with CCSD(T)/cc-pVQZ quadratic force constants. [d]Reference 39.

Table 4. Anharmonicity Constants (cm^{-1}) for CH_2D_2

anh	aVDZ[a]	aVTZ[b]	LMT[c]	exptl[d]	anh	aVDZ[a]	aVTZ[b]	LMT[c]	exptl[d]
x_{11}	−29.626	−27.388	−27.344	−25.304	x_{39}	0.897	0.288	0.651	−0.183
x_{12}	−1.177	−0.491	−0.831	−3.294	x_{44}	−3.859	−5.824	−4.492	−5.207
x_{13}	−11.501	−5.988	−7.251	−15.235	x_{45}	0.905	0.031	0.512	1.470
x_{14}	−2.286	−1.979	−2.052	−2.422	x_{46}	−1.400	−1.168	−1.411	−1.138
x_{15}	−12.058	−11.654	−11.752	−11.752	x_{47}	0.841	0.873	0.727	−0.868
x_{16}	−124.576	−115.395	−115.079	−114.112	x_{48}	−14.719	−15.207	−15.620	−15.620
x_{17}	−8.930	−8.969	−8.786	−7.765	x_{49}	−1.834	−2.448	−1.914	−2.571
x_{18}	0.188	0.570	0.403	−9.216	x_{55}	−1.629	−2.638	−2.211	−2.648
x_{19}	−6.811	−6.306	−6.139	−0.621	x_{56}	−13.209	−12.404	−12.869	−11.912
x_{22}	−15.326	−14.169	−14.130	−10.451	x_{57}	0.079	−1.712	0.385	0.385
x_{23}	−2.081	−1.990	−2.065	−3.609	x_{58}	−8.898	−9.585	−9.655	−9.655
x_{24}	−2.007	1.949	0.849	−0.568	x_{59}	−8.099	−10.880	−8.755	−9.671
x_{25}	−7.291	−7.334	−7.320	−7.320	x_{66}	−33.853	−31.657	−31.640	−31.566
x_{26}	−0.982	−0.080	−0.509	−0.509	x_{67}	−12.082	−11.120	−11.273	−11.062
x_{27}	−7.779	−7.990	−8.016	−1.750	x_{68}	3.567	4.113	3.715	3.715
x_{28}	−64.835	−60.029	−59.737	−58.073	x_{69}	−10.975	−11.015	−10.822	−12.732
x_{29}	−4.485	−4.534	−4.344	−7.677	x_{77}	−2.019	−2.530	−1.879	−6.587
x_{33}	−5.445	−8.505	−6.733	−5.191	x_{78}	−6.276	−7.246	−7.001	−7.001
x_{34}	−1.398	−2.395	−1.539	−1.983	x_{79}	3.021	0.814	3.590	2.464
x_{35}	0.248	−0.661	−0.447	−0.447	x_{88}	−19.821	−18.628	−18.583	−15.257
x_{36}	−21.898	−22.396	−22.147	−21.507	x_{89}	−8.708	−8.606	−15.620	−9.145
x_{37}	−6.948	−8.143	−7.529	−7.307	x_{99}	−4.321	−5.378	−4.354	−5.258
x_{38}	−3.066	−3.020	−3.067	−3.903					

[a]Present work; CCSD(T)/aVDZ level of theory. [b]Present work; CCSD(T)/aVTZ level of theory. [c]Reference 28; CCSD(T)/cc-pVTZ level of theory. [d]Reference 39.

computed without lowering the symmetry and the results can be compared to literature values more easily.

In Tables 3 and 4, experimental and theoretical vibrational constants for CH_2D_2 taken from the literature are compared with values computed in the present work. The harmonic frequencies obtained in the present work at the CCSD(T)/aVTZ level of theory agree with the experimental values[39] within about 10 cm^{-1}, as shown in Table 3. Theoretical calculations of LMT at the CCSD(T)/cc-pVQZ level of theory[28] demonstrate that even better agreement with experiment is obtained when a larger basis set is used. Our choice of the aVTZ basis set is a compromise between computational speed and accuracy for transition states. Our unpublished work suggests that, for transition states, augmented basis sets converge to the CBS limit faster than nonaugmented ones.[27]

The anharmonicities were computed using CFOUR at the CCSD(T) level of theory with two basis sets: aVDZ and aVTZ. The contributions of the anharmonicity and G_0 differ for the two basis sets, affecting the anharmonic zero point energies (ZPE_{anh}) as shown in Table 2. Calculations with even larger basis sets would be needed to estimate the CBS limit, but such very expensive calculations are beyond the scope of the present work. In Table 4, the anharmonicities computed in the present work for CH_2D_2 at the CCSD(T)/aVTZ level of theory are seen to be in good agreement with the calculations of LMT, who used a larger basis set; our calculations at the CCSD(T)/aVDZ level of theory are not as good, which has implications for the calculated KIEs, as discussed below. The calculated fundamental frequencies (Table 4) and corresponding zero point energies (Table 2), which must be taken into account

dx.doi.org/10.1021/jp212383u | J. Phys. Chem. A XXXX, XXX, XXX−XXX

when rate constants are computed, reflect the different basis sets.

Diagonal Born−Oppenheimer corrections are summarized in The Supporting Information. Reaction corrections (Δ_{DBOC}) obtained at the HF/aVTZ level of theory for Cl + CH_4 are ∼10 cm^{-1} larger than those obtained at the CCSD/aVTZ level. If DBOC corrections for other isotopic reactions are in error by this amount, the computed absolute rate constants could be in error by up to ∼5% at 298 K. However, most of this potential error is expected to cancel when KIEs are computed. This is an area of possible future improvements but is beyond the scope of the present work.

Absolute Rate Constants. Absolute rate constants for Cl + CH_4 are shown in Figure 1 and tabulated in the Supporting Information. As described above, the classical barrier height was taken from the work of Eskola et al.[24] Anharmonic vibrational and rotational constants for all species were obtained in the present work. Adiabatic corrections to the rate constant were based on the DBOC computed at the CCSD/aVTZ level of theory. The ab initio results for ^{35}Cl + $^{12}CH_4$ are in excellent agreement with the experimental data.[40−48] As discussed below and shown in Figure 2, the $^{35}Cl/^{37}Cl$ KIE is nearly equal to unity and thus the rate constant involving ^{35}Cl is almost identical with that involving the natural isotopic chlorine abundance. The ab initio rate constant for ^{35}Cl + $^{12}CH_4$ (Figure 1), which was computed using the TcTc data set (our best), is a little low compared to the experimental data at low temperatures and slightly high at high temperatures. The largest discrepancy (about 30%) is near 1100 K. Around 200 K, the ab initio rate constant is only ∼10% lower than the average data. At 298 K, the ab initio rate constant equals 0.948 × 10^{-13} cm^3 s^{-1}, which can be compared to the value of 1.0 × 10^{-13} cm^3 s^{-1} (±5%), which is recommended in critical data evaluations.[2,3] This excellent level of agreement is somewhat fortuitous because the CBS extrapolation method used by Eskola et al. has an intrinsic uncertainty of up to about ±2 kJ/mol. In this particular case, the apparent error is ∼0.13 kJ/mol.

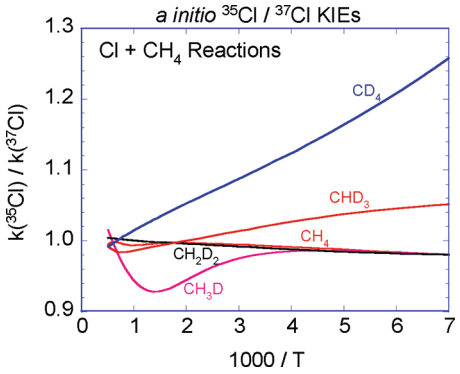

Figure 2. Chlorine ab initio KIEs for reaction with $^{12}CH_4$ and the H/D isotopologues. SCTST rate constants were computed using the TgDc data set with DBOC computed at the HF/aVTZ level of theory.

Unless otherwise noted, the TgDc data set and the DBOC computed at the HF/aVTZ level of theory were used for the isotopic calculations that follow. The absolute rate constant for Cl + CH_4 obtained using these parameters is 0.727 × 10^{-14} cm^3 s^{-1} at 298 K. This result is not quite as accurate as that obtained for the TcTc data set, but it is still in very good agreement with the experiments. Essentially exact agreement with the recommended experimental rate constant of 1.0 × 10^{-13} cm^3 s^{-1} can be obtained by empirically lowering the reaction barrier by only ∼0.8 kJ mol^{-1}, which is less than half the ∼2 kJ mol^{-1} maximum error expected for the extrapolation to the CBS limit.[24] This result is not as good as for the TcTc data set (discussed above) due to errors in the DBOC calculation, the anharmonicites, etc.

In the 1970s and 1980s, when most of the experiments were being carried out, curvature in the Arrhenius plot was cause for discussion and controversy. The ab initio rate constant shows distinct curvature in the Arrhenius plot. At lower temperatures, this is mostly due to quantum mechanical tunneling, which is included naturally in SCTST. The theory explicitly includes the effects of tunneling, curvature of the multidimensional reaction path, and coupling among all degrees of freedom, including the reaction coordinate. At high temperatures, the curvature in the Arrhenius plot is mostly due to the vibrational anharmonicity of CH_4, which includes coupling among all of the vibrational degrees of freedom. Other recent theoretical treatments of this reaction predict curvature in the Arrhenius plot,[49−51] although critical evaluations[2,3] still tend to state their recommendations in Arrhenius form.

In the late 1970s, it was noted that a systematic discrepancy appeared to exist between rate constants measured in discharge flow tubes and those measured in flash photolysis apparatus.[2] Ravishankara and Wine[44] investigated this effect systematically and showed that the discrepancy is related to gas mixture composition. They hypothesized that in experiments at temperatures below 300 K, the thermal equilibrium may not be maintained between $^2Cl_{1/2}$ and $^2Cl_{3/2}$. Equilibrium can be maintained despite the occurrence of chemical reaction when efficient collider gases and walls are present, but when the bulk gas is helium, which is an inefficient collider gas, thermal equilibrium is not maintained. This controversy has never been fully resolved and it will not be resolved by the present work, either. We merely note that our theoretical calculations assume that the two states are in thermal equilibrium and the predicted rate constants are in good agreement with the experiments over a very wide range of temperatures.

In Figure 3, three recent theoretical calculations of the rate constant for Cl + CH_4 are compared with the ab initio SCTST results computed in the present work. The CUS/μOMT calculations were carried out using the canonical unified statistical theory[49,52] (CUS) with microcanonical optimized multidimensional tunneling[53] (μOMT). Corchado et al.

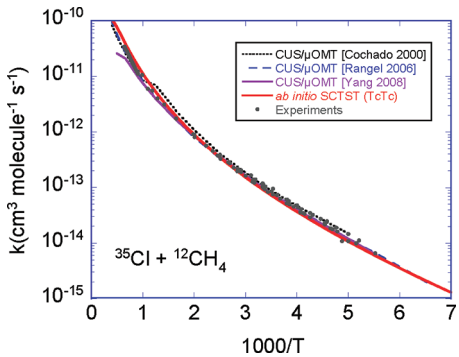

Figure 3. SCTST (TcTc) ab initio results compared to other recent theoretical treatments.[49−51] SCTST rate constants were computed using the TcTc data set with DBOC computed at the CCSD/aVTZ level of theory.

dx.doi.org/10.1021/jp212383u | J. Phys. Chem. A XXXX, XXX, XXX−XXX

developed an analytical potential energy surface (PES) that was calibrated empirically to fit the experimental rate constant and isotopic data. Their rate constant is in good agreement with the experimental data, although it exhibits changes in slope near 1000 K due to changes in the variationally determined transition state. The PES was modified and recalibrated some time later by Rangel et al., resulting in better agreement with the data and a reduction in the changes in slope at high temperatures.[50] Yang et al. modified and recalibrated the PES again, based on ab initio calculations at the CCSD(T)/aVTZ level of theory (as in the present work), obtaining slightly different results, especially at high temperatures, but still with the changes of slope seen in earlier calculations.[51]

The present ab initio SCTST calculations are presented in Figure 3 without any empirical adjustments. They are in very good agreement with the other theoretical calculations (and with the experimental data, as discussed above). They fall a little lower than the other calculations and the experimental data at low temperatures and slightly higher at high temperatures, but the differences are modest. The present calculations were carried out at a pragmatic level of theory. In principle they can be improved by utilizing larger basis sets and higher levels of theory. Nonetheless, the SCTST results are comparable in accuracy to the empirically calibrated theoretical calculations.

H/D KIEs for the Forward Reaction. The KIEs were calculated by taking ratios of ab initio rate constants. As discussed above, the ab initio rate constants do not match the experimental absolute rate constants exactly, but the barrier heights can be adjusted so that they will match. Test calculations showed that the KIEs computed with the ab initio and the empirically adjusted rate constants differed by <0.001. Thus only the ab initio rate constants (with no adjustments) were used to compute the KIEs in the present work.

Rate constants for ^{35}Cl and ^{37}Cl reacting with methane were computed for most of the C and H isotopic combinations and are tabulated in Supporting Information. KIEs for $^{35}Cl/^{37}Cl$ reacting with $^{12}CH_4$ and its H/D isotopologues are shown in Figure 2. The shapes of these curves are rather complex, because each KIE depends on anharmonic coupling among the vibrations of both the transition state and the methane reactant, in addition to quantum mechanical tunneling. To the best of our knowledge, the chlorine KIEs for the reaction with methane have never been measured.

The H/D KIEs have been reported by several research groups. The consistency among the measurements is fair to good, but only a few groups report the temperature dependence of the KIEs. The ab initio KIEs obtained in the present work are compared with experimental data and with a few selected theoretical calculations in Figures 4−7. Most of the theoretical calculations shown for comparison are based on the CUS/μOMT method,[49,52,53] which generally produces reasonably accurate results. The work by Corchado et al.[49] is a further development of the extensive earlier work reported by Roberto-Neto et al.[54] The work of Rangel et al. is a further improvement along the same lines.[50] Banks and Clary carried out a quantum dynamics simulation, based on a 2-D reduced dimensionality ab initio PES computed at the CCSD(T)/cc-pVTZ//MP2/cc-pVTZ level of theory and fitted to analytical functions.[55] Yang and co-workers have applied a quantum dynamical wave packet propagation method to the Cl + CH_4 reaction[51] and Cl + CD_4.[56] Other calculations are cited by these references and by other recent papers.[57,58]

Among the deuterated methane isotopologues, CH_3D is particularly important for atmospheric studies because it occurs in natural abundances that are accessible to accurate measurements. The multideuterated methane isotopologues occur in much lower abundances, because the natural D/H ratio is only 1.15×10^{-4}.[59] The experimental data displayed in Figure 4 is of

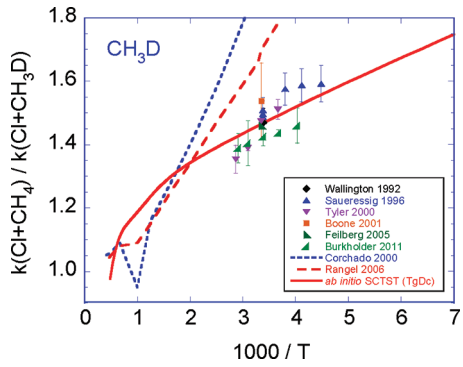

Figure 4. Kinetic isotope effects for Cl + CH_3D. Experimental data[57,60−62,66] are shown as points (2σ error bars), and the line is the ab initio KIE. The SCTST rate constants were computed using the TgDc data set and DBOC computed at the HF/aVTZ level of theory. The other lines are for calculated rate constants taken from the literature.[49,50]

fair consistency, but measurements from several groups do not agree within their nominal 2σ uncertainties. Note that the datum published by Wallington and Hurley[60] for this reaction was revised later and the revised value was reported by Saueressig et al.[61]

As shown in Figure 4, the ab initio KIEs computed with the TgDc data set pass through the cluster of data points measured by several groups near 300 K and are within ±5% of all of the experimental data points. The slope of the ab initio line is essentially parallel to the slopes of the data reported by Saueressig et al.[61] and Burkholder,[62] who provided us with the data reported at a Faraday Discussion meeting by Sauer et al.[63] The theoretical calculations reported by Corchado et al.[49] and the improved model of Rangel et al.[50] are not in good agreement with the experimental data and have a much stronger temperature dependence. They also exhibit the changes in slope near 1000 K that are due to abrupt switching between variationally determined transition states.

In Figure 5, additional comparisons are made between the data, SCTST and results from conventional canonical transition state theory (CTST) applied to ^{35}Cl + $^{12}CH_3D$. The CTST calculations were carried out using THERMO, part of the MultiWell Program Suite, using the identical harmonic frequencies and rotational constants used in the SCTST calculations. Quantum mechanical tunneling was included by assuming an unsymmetrical Eckart potential energy barrier and using the same imaginary frequency that was used in the SCTST calculations. The forward energy barrier was obtained as the sum of the classical energy plus the harmonic zero point energy. The results obtained using this conventional approach are shown in Figure 5 along with the literature data and the SCTST results, which also appear in Figure 4. The results presented in Figure 4 and Figure 5 show that among these computed rate constants, only SCTST predicts the KIE with accuracy comparable to that of the experiments.

dx.doi.org/10.1021/jp212383u | J. Phys. Chem. A XXXX, XXX, XXX−XXX

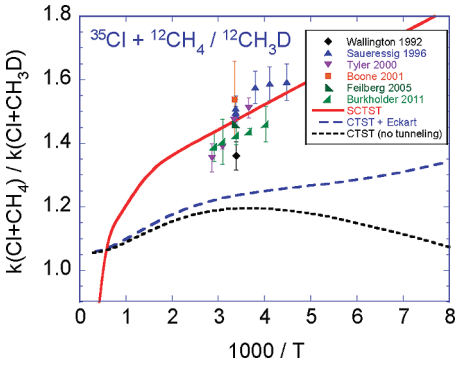

Figure 5. Kinetic isotope effects for Cl + CH_3D. Experimental data[57,60−62,66] are shown as points (2σ error bars). The ab initio SCTST rate constants were computed using the TgDc data set and DBOC computed at the HF/aVTZ level of theory. The ab initio conventional CTST rate constants (with and without tunneling) were calculated in this work with the same ab initio parameters, as described in the text.

Experimental data and theoretical calculations for Cl + CH_2D_2 are presented in Figure 6. The ab initio KIEs are within

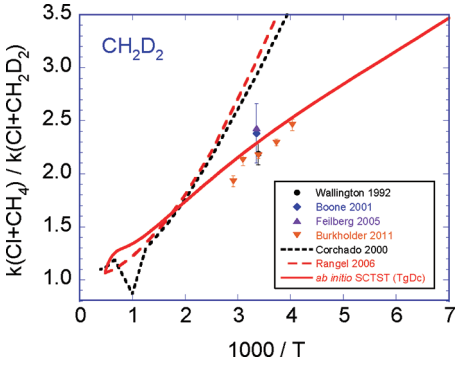

Figure 6. Kinetic isotope effects for Cl + CH_2D_2. Experimental data[57,60,62,66] are shown as points (2σ error bars), and the line is the ab initio KIE. The SCTST rate constants were computed using the TgDc data set and DBOC computed at the HF/aVTZ level of theory.

±5% of most of the experimental data points, although some differ by as much as ∼10%. The theoretical line passes right between two groups of experimental data at ∼300 K. It seems likely that the theoretical errors are ∼5% or less. At temperatures above 1000 K, the ab initio line exhibits a "wiggle" (also apparent in Figures 6 and 7). Near 2000 K, some of this effect may be due to truncating the Boltzmann distribution at 20 000 cm^{-1}, as discussed above. For this reason, errors in the SCTST results near 2000 K are probably larger ... perhaps ±10%. The CUS/μOMT calculations reported by Corchado et al.[49] and Rangel et al.[50] do not agree very well with either the magnitude or the temperature dependence of the experimental KIEs.

The experimental KIEs for CHD_3 are more limited than for the other isotopomers. The data are presented along with theoretical calculations in Figure 7. For this case, the ab initio SCTST results are ∼25% higher than the measurements of Burkholder et al.,[62] ∼10% higher than the results of Wallington and Hurley,[60] but in almost perfect agreement with the results of Feilberg et al.[57] Considering the lack of agreement among the measurements, it is impossible to reach any firm conclusions about the performance of SCTST for this

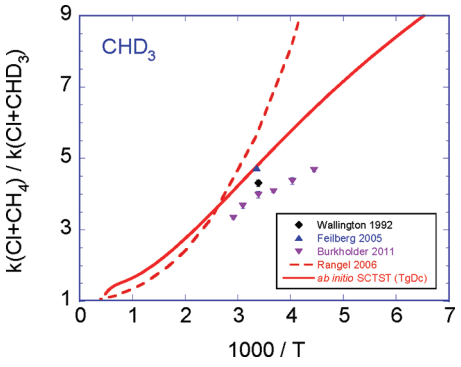

Figure 7. Kinetic isotope effects for Cl + CHD_3. Experimental data[57,60,62] are shown as points (2σ error bars), and the line is the ab initio KIE. The SCTST rate constants were computed using the TgDc data set and DBOC computed at the HF/aVTZ level of theory.

isotopologue. The theoretical results of Rangel et al.[50] are not in good agreement with the experimental data, although they converge with the present ab initio SCTST results at temperatures above ∼350 K.

CD_4 has been a popular subject of both calculations and measurements, which are shown in Figure 8. The ab initio

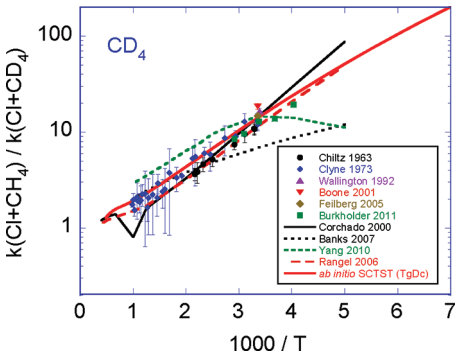

Figure 8. Kinetic isotope effects for Cl + CD_4. Experimental data[57,60,62,66−68] are shown as points (2σ error bars), and the line is the ab initio KIE. The SCTST rate constants were computed using the TgDc data set and DBOC computed at the HF/aVTZ level of theory. Other theoretical rate constants from the literature are shown as lines.

SCTST results fall in the midst of the experimental data. Most of the experimental data are within ∼15% of the calculated line over the entire range of temperatures that have been investigated. Because the theoretical line passes through the midst of the collection of experimental data, it seems likely that the theoretical errors are ∼10% or less. Except for the changes in slope at high temperatures, the calculations of Corchado et al.[49] and Rangel et al.[50] are also in very good agreement with the experimental data. The quantum dynamics calculation of Yang et al.[56] gave KIEs that are systematically a little higher than the experiments at temperatures from 300 to 1000 K, but pass through a maximum at 300 K and strangely decrease at lower temperatures. The results of Banks and Clary[55] are in fair agreement with the experiments but show a weaker temperature dependence.

H/D KIEs for the Reverse Reaction. The absolute rate constants for the reverse reaction (i.e., CH_3 + HCl) have been

dx.doi.org/10.1021/jp212383u | J. Phys. Chem. A XXXX, XXX, XXX−XXX

measured by Russell et al.[64] and Eskola et al.,[65] but only the latter have measured KIEs. The reactions are as follows:

$$CH_3 + HCl \rightarrow CH_4 + Cl \quad (a)$$

$$CH_3 + DCl \rightarrow CH_3D + Cl \quad (b)$$

$$CD_3 + HCl \rightarrow CHD_3 + Cl \quad (c)$$

$$CD_3 + DCl \rightarrow CD_4 + Cl \quad (d)$$

The measured KIEs of Eskola et al. (their Table 2) and those computed in the present work using ab initio SCTST are defined as follows and are presented in Figure 9.

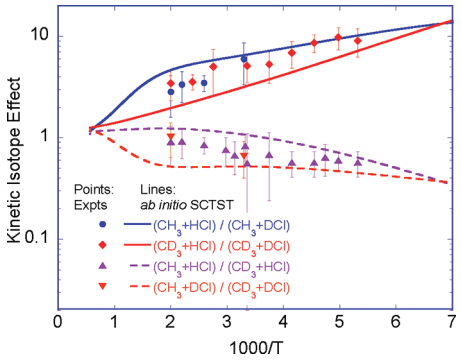

Figure 9. Kinetic isotope effects for isotopologues of CH_3 + HCl. Experimental data[65] are shown as points (2σ error bars), and all lines were computed using ab initio SCTST with the TgDc data set and DBOCs computed at the HF/aVTZ level of theory.

$$KIE(1) = \frac{k_a}{k_b} \qquad KIE(2) = \frac{k_c}{k_d} \qquad KIE(3) = \frac{k_a}{k_c}$$

$$KIE(4) = \frac{k_b}{k_d} \quad (12)$$

KIE(1) and KIE(2) depend mostly on the primary isotope effect, which refers to the actual transfer of an H or D atom. However, both KIEs are also modified by the secondary isotope effect, which depends on the identity of the spectator group, i.e., CH_3 or CD_3. In agreement with the experimental data of Eskola et al, the ab initio SCTST calculations predict that KIE(1) and KIE(2) increase as the temperature decreases. However, unlike the experimental data, the calculations predict that the KIE(1) and KIE(2) first diverge from each and then converge again as the temperature decreases, producing a maximum difference near 500 K. The experimental KIEs do not seem to diverge from each other at any temperature, although this conclusion is only tentative, because of the size of the error bars and because only four experimental data points were reported for KIE(1).[65]

Similar comments can be made about KIE(3) and KIE(4), which are mostly sensitive to the secondary isotope effect. Note that only two data points are reported for KIE(4).[65] Because zero point energy differences for the secondary isotope effects are not as great as for primary isotope effects, these KIEs are almost independent of temperature. For all of the data, the typical differences from the theory are approximately ±50%, and the experimental error bars are relatively large.

$^{12}C/^{13}C$ and $^{12}C/^{14}C$ KIEs for the Forward Reaction. The carbon KIEs are much smaller than the H/D KIEs, because the relative change in mass is much smaller. The experimental $^{12}C/^{13}C$ KIEs are plotted in Figure 10 as points (2σ error bars) and the theoretical $^{12}C/^{13}C$ and $^{12}C/^{14}C$ KIEs are presented as lines.

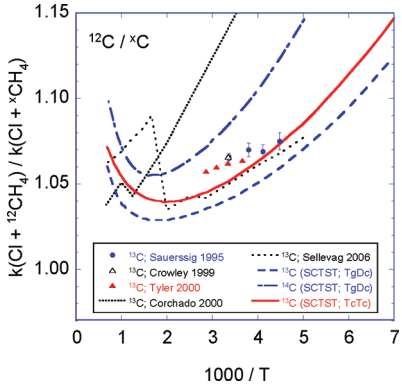

Figure 10. ^{13}C and ^{14}C kinetic isotope effects for Cl + CH_3. Experimental data[69−71] are shown as points (2σ error bars), the dotted lines are the calculated KIEs of Corchado et al.[49] and Sellevåg et al.,[58] and the dashed lines are the present SCTST results. The SCTST rate constants were computed using the TgDc or TcTc data sets, and DBOC, at the HF/aVTZ or CCSD/aVTZ level of theory.

The experimental data are reasonably consistent, although the differences between data sets are in some cases greater than the combined error bars. The COS/μOMT calculations of Corchado et al.[49] are much higher than the experimental data and at high temperatures show some effects of switching between variationally determined transition states. The (scaled) CUS with small curvature tunneling calculations of Sellevåg et al. are in much better agreement with the data, although the changes in slope at high temperatures are more pronounced.[58] The results of Sellevåg et al. at moderate temperatures are fortuitously in close agreement with the results obtained using SCTST in a special calculation, as described below.

The ab initio SCTST results for $^{12}C/^{13}C$ and $^{12}C/^{14}C$ KIEs shown by broken lines were computed using the same level of vibrational data (TgDc) that was used for computing the H/D KIEs. The $^{12}C/^{13}C$ KIEs from the TgDc vibrational data set provide an example of good news/bad news. The good news is that the ratio of the ab initio rate constants computed using SCTST differs from the experimental data by only about 2%: this level of performance is excellent. The bad news is *also* that the ratio of the ab initio rate constants computed using SCTST differ from the experimental data by about 2%: this margin of difference is too large for serviceable predictions of these small KIEs. After all, one goal of carrying out calculations such as these is to provide predictions that are useful for analyzing atmospheric isotopic composition.

Below ~500 K, the slopes of the $^{12}C/^{13}C$ and $^{12}C/^{14}C$ KIE plots are negative, but they reverse sign at higher temperatures.

dx.doi.org/10.1021/jp212383u | J. Phys. Chem. A XXXX, XXX, XXX−XXX

To analyze this behavior, we express KIE in the a form that is familiar from transition state theory:

$$\mathrm{KIE} = \frac{k_{\mathrm{Cl}+^{12}\mathrm{CH_4}}}{k_{\mathrm{Cl}+^{13}\mathrm{CH_4}}} = \left[\left(\frac{q_{12}}{q_{13}}\right)_{\mathrm{rot}}\left(\frac{q_{12}}{q_{13}}\right)_{\mathrm{vib}}\right]_{\ddagger}\left[\left(\frac{q_{13}}{q_{12}}\right)_{\mathrm{vib}}\left(\frac{q_{13}}{q_{12}}\right)_{\mathrm{trans}}\right]_{\mathrm{CH_4}} \times \exp(-\Delta(\Delta E_z)/k_B T) \quad (13)$$

where ratios of partition functions for rotation and vibration of the transition state isotopomers and of methane isotopologues are given in the square brackets. Relative translation between Cl and CH_4 isotopologues is also included. Note that the vibrational partition function for the transition state is actually the partition function of the vibrational part of the cumulative reaction probability, which includes the effects of anharmonicity and quantum mechanical tunneling. For partition functions evaluated relative to the zero point energy of each species, $\Delta(\Delta E_z)$ is the difference in the reaction zero point energy differences (or, equivalently, the difference in the zero point energy corrected critical energies for the reactions). The classical barrier height and the partition functions for Cl atom and methane rotations cancel out and therefore do not appear in the equation.

To determine the sources of the temperature dependence, each factor in eq 13 can be evaluated from the data summarized in the Supporting Information. The difference in reaction zero point energy differences, $\Delta(\Delta E_z)$, is <1 cm^{-1}, which is insignificant. Because both transition states have C_{3v} symmetry and the carbon atom lies on the symmetry axis, only the 2-D rotations remain without cancellation. The appropriate rotational constants for the transition states are B_{12} = 0.1875 cm^{-1} and B_{13} = 0.1799 cm^{-1} for ^{12}C and ^{13}C labeled transition states, respectively. Within the classical approximation, the ratio of rotational partition functions is $[q^{\ddagger}_{12}/q^{\ddagger}_{13}]_{\mathrm{rot}} = B_{13}/B_{12}$, which is independent of temperature. The ratio of quantum rotational partition functions, which is required for better accuracy at low temperatures, depends weakly on temperature, but the effect is very small. Similarly, the ratio of translational partition functions is also independent of temperature. Thus the temperature dependence must originate from the remaining two factors, which involve vibrations.

The two remaining factors in eq 13 involve anharmonic vibrations in methane and a combination of anharmonic vibrations and quantum mechanical tunneling in the transition state. These factors are shown as a function of $1000/T$ in Figure 11. The results show that the ratio of vibrational functions for methane increases weakly with temperature. The result for the transition state show significant effects at both low and high temperatures and strongly resembles the KIEs shown in Figure 10. At low temperatures, quantum mechanical tunneling is dominant, resulting in a dramatic increase in $[q^{\ddagger}_{12}/q^{\ddagger}_{13}]_{\mathrm{vib}}$ at temperatures below ~500 K. At higher temperatures, where tunneling contributions should be decreasing steadily, $[q^{\ddagger}_{12}/q^{\ddagger}_{13}]_{\mathrm{vib}}$ increases again. This behavior is most likely due to anharmonic vibrational coupling causing $q^{\ddagger}_{12}$ to increase more rapidly than $q^{\ddagger}_{13}$ with increasing temperatures. The methane partition function ratio reinforces this effect, leading to the sharp increase in KIEs at temperatures greater than 500 K.

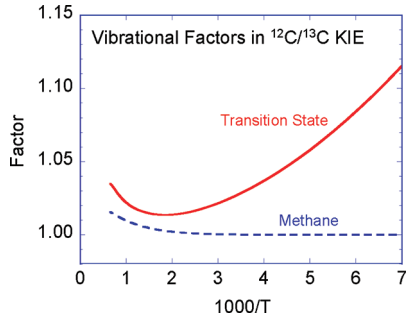

Figure 11. Contributions of the vibrational factors in the $^{12}C/^{13}C$ kinetic isotope effect (based on the TgDc data set). The curves labeled "Transition State" and "Methane" are the second and third factors, respectively, in square brackets on the right-hand side of eq 13.

The principal conclusion from this analysis is that quantum mechanical tunneling and vibrational anharmonicity in the transition state are both important in determining kinetic isotope effects, and they respond to temperature differently, more or less as expected. Methane anharmonicity plays a smaller role but reinforces the effect.

Errors and Improvements. From the discussion in the previous sections, it is clear that estimating the errors in the ab initio SCTST KIEs is not straightforward. The high quality of the ab initio rate constants (aside from possible errors in the reaction energy barrier) argues for the quality of the computed KIEs. An important limitation in comparing theory with experiments is that the experimental measurements are somewhat inconsistent. In most cases, however, the calculated KIEs fall in the midst of the experimental measurements, suggesting that they are of comparable accuracies. For the H/D KIEs in the forward direction, the errors appear to be random and thus the inherent accuracy of the calculations may be significantly smaller than the average 5−15% differences from the scattered data points. We estimate that the relative intrinsic errors in the H/D KIEs are ~5%, or less. This conclusion is supported indirectly by the fact that the $^{12}C/^{13}C$ KIEs at 300 K are in error by only 2%.

For the reverse direction, systematic discrepancies are apparent. The average differences between experiment and theory are ~50%. It is not clear why the calculations are more seriously in error for the reverse direction. It is possible that using the improvements described below will reduce the errors. It is desirable that the KIEs in the reverse direction be confirmed by additional experiments.

During the course of this work, we have identified several possible ways of improving the accuracy of the calculations, but only at an additional cost. The first improvement is to use a larger basis set to obtain vibrational parameters closer to the CBS limit. To reduce computational costs, we used the aVTZ basis set for computing harmonic frequencies and the aVDZ basis set for computing anharmonicity coefficients (the TgDc set). We also computed the DBOC at a low level of theory (HF/aVTZ), because the corrections are relatively small. However, these shortcuts potentially introduce errors that may not cancel out when the KIEs are computed. The 2% relative error at in the $^{12}C/^{13}C$ KIEs at 300 K could be due to an energy error of only 4 cm^{-1}.

To determine whether better results can be achieved for the $^{12}C/^{13}C$ KIEs by reducing the shortcuts, we computed the TcTc vibrational data sets for the two reaction systems: ^{35}Cl + $^{12}CH_4$ and ^{35}Cl + $^{13}CH_4$. Although they are small, the DBOCs

dx.doi.org/10.1021/jp212383u | J. Phys. Chem. A XXXX, XXX, XXX−XXX

were computed for these species using the CCSD/aVTZ level of theory, which is considerably higher than before. The ab initio $^{12}C/^{13}C$ KIEs computed with SCTST using these data are presented in Figure 10 as the solid red line, which is practically coincident with the theoretical calculations of Sellevåg et al.[58] and is in error by only ~1% (the temperature dependence is slightly different from the experiments). This improvement in performance suggests that using still larger basis sets and higher levels of theory is likely to improve the results to the point where they will be genuinely useful for analyzing environmental data.

Additional KIEs. In addition to the results presented in the text of this paper, additional ab initio KIEs involving other combinations of Cl, C, and H isotopes can be calculated from the ab initio SCTST rate constants tabulated in the Supporting Information. These include reactions such as

$$^{35}Cl + {}^{13}CH_3D \rightarrow H^{35}Cl + {}^{13}CH_2D \quad (14)$$

$$^{35}Cl + {}^{13}CH_3D \rightarrow D^{35}Cl + {}^{13}CH_3 \quad (15)$$

CONCLUSIONS

The main motivation for this work was to determine whether SCTST can produce ab initio KIEs of sufficient accuracy to be useful in analyzing atmospheric isotopic composition. For H/D KIEs the answer is an emphatic affirmative. The errors in the theoretical calculations appear to be about the same as, or less than, the errors in the experiments. For $^{12}C/^{13}C$ KIEs, the results are very good, but probably still not satisfactory at the levels of theory used in the present work. However, tests with a larger basis set suggest the results can be improved systematically, which makes it a very promising method. In addition, the absolute rate constants (which were of secondary interest in this work) are predicted accurately as well. SCTST performs as well as or better than other theories in predicting H/D KIEs when a pragmatic level of theory is used for obtaining the required vibrational data.

The ultimate goal of this work is to develop theoretical methods that are as accurate as experimental data, so that the theoretical results can be used with confidence when experimental data do not exist. The present work is a step along that path.

ASSOCIATED CONTENT

Supporting Information

Optimized geometries, harmonic and anharmonic vibrational constants, rotational constants, and DBOCs (computed at various levels of theory and for various basis sets) are tabulated for all species and transition states. Reaction barriers in the forward and reverse directions (including anharmonic zero point energies computed using the TgDc data set) are also tabulated. In addition, ab initio SCTST rate constants for individual isotopic reaction channels, total rate constants for the natural abundance of Cl, and kinetic isotope effects are tabulated for temperatures from ~100 to 2000 K. This material is available free of charge via the Internet at http://pubs.acs.org.

AUTHOR INFORMATION

Corresponding Author

*E-mail: J.R.B., jrbarker@umich.edu; J.F.S., jfstanton@mail.utexas.edu.

Notes

The authors declare no competing financial interest.

§E-mail: nguyenlt@umich.edu.

ACKNOWLEDGMENTS

We thank A. R. Ravishankara for several interesting and insightful discussions of the relative merits of theory and experiment. We thank James B. Burkholder for providing us with the data that were the basis for the conference paper presented by Sauer et al.[63] J.R.B. and T.L.N. thank the National Science Foundation (Atmospheric and Geospace Sciences) and NASA (Upper Atmospheric Research Program), and J.F.S. thanks the Robert A. Welch Foundation (Grant F-1283) and the National Science Foundation for support of this research.

REFERENCES

(1) *IPCC Climate Change 2007: The Physical Science Basis, Contribution of Working Group I to the Fourth Assessment Report of the Intergovernmental Panel on Climate Change*; Cambridge University Press: Cambridge, U.K., and New York, NY, U.S.A., 2007.

(2) Sander, S. P.; Abbatt, J.; Barker, J. R.; Burkholder, J. B.; Friedl, R. R.; Golden, D. M.; Huie, R. E.; Kolb, C. E.; Kurylo, M. J.; Moortgat, G. K.; Orkin, V. L.; Wine, P. H. *Chemical Kinetics and Photochemical Data for Use in Atmospheric Studies, Evaluation Number 17*; JPL Publication 10-6; Jet Propulsion Laboratory, Pasadena, 2011.

(3) Atkinson, R.; Baulch, D. L.; Cox, R. A.; Crowley, J. N.; Hampson, R. F.; Hynes, R. G.; Jenkin, M. E.; Rossi, M. J.; Troe, J. *Atmos. Chem. Phys.* **2006**, *6*, 3625−4055.

(4) Stevens, C. M.; Rust, F. E. *J. Geophys. Res.* **1982**, *87*, 4879−4882.

(5) Gupta, M.; Tyler, S.; Cicerone, R. *J. Geophys. Res.* **1996**, *101*, D22,923−D922,932.

(6) Rice, A. L.; Tyler, S. C.; McCarthy, M. C.; Boering, K. A.; Atlas, E. *J. Geophys. Res.* **2003**, *108*, 4460.

(7) Tyler, S. C.; Rice, A. L.; Ajie, H. O. *J. Geophys. Res.* **2007**, *112*, D03303 (03316 pages).

(8) Röckmann, T.; Brass, M.; Borchers, R.; Engel, A. *Atmos. Chem. Phys. Discuss.* **2011**, *11*, 12039−12102.

(9) Brownlow, A. H. *Geochemistry*, 2nd ed.; Prentice-Hall, Inc.: Upper Saddle River, NJ, 1996.

(10) Johnson, M. S.; Feilberg, K. L.; Hessberg, P. v.; Nielsen, O. *J. Chem. Soc. Rev.* **2002**, *31*, 313−323.

(11) Brenninkmeijer, C. A. M.; Janssen, C.; Kaiser, J.; Röckmann, T.; Rhee, T. S.; Assonov, S. S. *Chem. Rev.* **2003**, *103*, 5125−5161.

(12) Weston, R. E. Jr. *Chem. Rev.* **1999**, *99*, 2115−2136.

(13) Miller, W. H. *Faraday Discuss. Chem. Soc.* **1977**, *62*, 40−46.

(14) Miller, W. H.; Hernandez, R.; Handy, N. C.; Jayatilaka, D.; Willets, A. *Chem. Phys. Lett.* **1990**, *172*, 62−68.

(15) Cohen, M. J.; Handy, N. C.; Hernandez, R.; Miller, W. H. *Chem. Phys. Lett.* **1992**, *192*, 407−416.

(16) Hernandez, R.; Miller, W. H. *Chem. Phys. Lett.* **1993**, *214*, 129−136.

(17) Nguyen, T. L.; Stanton, J. F.; Barker, J. R. *Chem. Phys. Lett.* **2010**, *499*, 9−15.

(18) Nguyen, T. L.; Stanton, J. F.; Barker, J. R. *J. Phys. Chem. A* **2011**, *115*, 5118−5126.

(19) J. F. Stanton, J. Gauss, M. E. Harding, P. G. Szalay, w. c. f. A. A. Auer, ; R. J. Bartlett, U. Benedikt, C. Berger, D. E. Bernholdt, Y. J. Bomble, O. Christiansen, M. Heckert, O. Heun, C. Huber, T.-C. Jagan, D. Jonsson, J. Jusélius, K. Klein, W. J. Lauderdale, D. A. Matthews, T. Metzroth, D. P. O'Neill, D. R. Price, E. Prochnow, K. Ruud, F. Schiffmann, S. Stopkowicz, J. Vázquez, F. Wang, J. D. Watts and the integral packages MOLECULE (J. Almlöf, P.R. Taylor); PROPS (P.R. Taylor); ABACUS (T. Helgaker, H. J. Aa. Jensen, P. Jørgensen, J.Olsen); and ECP routines by A. V. Mitin, C. van Wüllen. CFOUR. In a quantum chemical program package, 2009.

(20) Mills, I. M. Vibration-Rotation Structure in Asymmetric- and Symmetric-Top Molecules. In *Molecular Spectroscopy: Modern*

Research; Rao, K. N., Mathews, C. W., Eds.; Academic Press: New York, 1972; Vol. *1*; pp 115−140.
(21) Tajti, A.; Szalay, P. G.; Csaszar, A. G.; Kallay, M.; Gauss, J.; Valeev, E. F.; Flowers, B. A.; Vazquez, J.; Stanton, J. F. *J. Chem. Phys.* **2004**, *121*, 11599−11613.
(22) Bomble, Y. J.; Vazquez, J.; Kallay, M.; Michauk, C.; Szalay, P. G.; Csaszar, A. G.; Gauss, J.; Stanton, J. F. *J. Chem. Phys.* **2006**, *125*, 064108.
(23) Harding, M. E.; Vazquez, J.; Ruscic, B.; Wilson, A. K.; Gauss, J.; Stanton, J. F. *J. Chem. Phys.* **2008**, *128*, 114111.
(24) Eskola, A. J.; Timonen, R. S.; Marshall, P.; Chesnokov, E. N.; Krasnoperov, L. N. *J. Phys. Chem. A* **2008**, *112*, 7391−7401.
(25) Raghavachari, K.; Trucks, G. W.; Pople, J. A.; Head-Gordon, M. *Chem. Phys. Lett.* **1989**, *157*, 479.
(26) *Electronic Spin Splitting Corrections, Computational Chemistry Comparison and Benchmark DataBase*, Release 15b, August 2011 ed.; NIST Standard Reference Database 101; National Institute of Standards and Technology: Gaithersburg, MD, 2011, http://cccbdb.nist.gov/.
(27) Barker, J. R.; Nguyen, T. L.; Stanton, J. F. Application of Semi-Classical Transition State Theory to Thermal and Non-Thermal Reaction Rates. In *7th International Conference on Chemical Kinetics*; Massachusetts Institute of Technology: Cambridge, MA, 2011.
(28) Lee, T. J.; Martin, J. M. L.; Taylor, P. R. *J. Chem. Phys.* **1995**, *102*, 254−261.
(29) Frisch, M. J.; Trucks, G. W.; Schlegel, H. B.; Scuseria, G. E.; Robb, M. A.; Cheeseman, J. R.; Scalmani, G.; Barone, V.; Mennucci, B.; Petersson, G. A.; Nakatsuji, H.; Caricato, M.; Li, X.; Hratchian, H. P.; Izmaylov, A. F.; Bloino, J.; Zheng, G.; Sonnenberg, J. L.; Hada, M.; Ehara, M.; Toyota, K.; Fukuda, R.; Hasegawa, J.; Ishida, M.; Nakajima, T.; Honda, Y.; Kitao, O.; Nakai, H.; Vreven, T.; J. A. Montgomery, J.; Peralta, J. E.; Ogliaro, F.; Bearpark, M.; Heyd, J. J.; Brothers, E.; Kudin, K. N.; Staroverov, V. N.; Kobayashi, R.; Normand, J.; Raghavachari, K.; Rendell, A.; Burant, J. C.; Iyengar, S. S.; Tomasi, J.; Cossi, M.; Rega, N.; Millam, J. M.; Klene, M.; Knox, J. E.; Cross, J. B.; Bakken, V.; Adamo, C.; Jaramillo, J.; Gomperts, R.; Stratmann, R. E.; Yazyev, O.; Austin, A. J.; Cammi, R.; Pomelli, C.; Ochterski, J. W.; Martin, R. L.; Morokuma, K.; Zakrzewski, V. G.; Voth, G. A.; Salvador, P.; Dannenberg, J. J.; Dapprich, S.; Daniels, A. D.; Farkas, O.; Foresman, J. B.; Ortiz, J. V.; Cioslowski, J.; Fox, D. J. *Gaussian 09*, Revision A.1; Gaussian, Inc.: Wallingford, CT, 2009.
(30) Miller, W. H. *J. Chem. Phys.* **1975**, *62*, 1899−1906.
(31) Truhlar, D. G.; Isaacson, A. D. *J. Chem. Phys.* **1990**, *94*, 357−359.
(32) Wang, F.; Landau, D. P. *Phys. Rev. Lett.* **2001**, *86*, 2050−2053.
(33) Basire, M.; Parneix, P.; Calvo, F. *J. Chem. Phys.* **2008**, *129*, 081101.
(34) Nguyen, T. L.; Barker, J. R. *J. Phys. Chem. A* **2010**, *114*, 3718−3730.
(35) Barker, J. R. *Int. J. Chem. Kinetics* **2001**, *33*, 232−245.
(36) Barker, J. R.; Ortiz, N. F.; Preses, J. M.; Lohr, L. L.; Maranzana, A.; Stimac, P. J.; Nguyen, T. L.; Kumar, T. J. D. *MultiWell-2011.3 Software*; Barker, J. R., Ed.; University of Michigan: Ann Arbor, Michigan, U.S.A., 2011; http://aoss.engin.umich.edu/multiwell/.
(37) Mielke, S. L.; Peterson, K. A.; Schwenke, D. W.; Garrett, B. C.; Truhlar, D. G.; Michael, J. V.; Su, M.-C.; Sutherland, J. W. *Phys. Rev. Lett.* **2003**, *91*, 063201.
(38) Coursey, J. S.; Schwab, D. J.; Tsai, J. J.; Dragoset, R. A. *Atomic Weights and Isotopic Compositions* (version 3.0). [Online]; National Institute of Standards and Technology: Gaithersburg, MD, 2010, http://physics.nist.gov/Comp.
(39) Ulenikov, O. N.; Bekhtereva, E. S.; Albert, S.; Bauerecker, S.; Hollenstein, H.; Quack, M. *J. Phys. Chem. A* **2009**, *113*, 2218−2231.
(40) Manning, R.; Kurylo, M. J. *J. Phys. Chem.* **1977**, *81*, 291−296.
(41) Whytock, D. A.; Lee, J. H.; Michael, J. V.; Payne, W. A.; Stief, L. J. *J. Chem. Phys.* **1977**, *66*, 2690−2695.
(42) Keyser, L. F. *J. Chem. Phys.* **1978**, *69*, 214−218.
(43) Zahniser, M. S.; Berquist, B. M.; Kaufman, F. *Int. J. Chem. Kinet.* **1978**, *10*, 15−29.
(44) Ravishankara, A. R.; Wine, P. H. *J. Chem. Phys.* **1980**, *72*, 25−30.
(45) Heneghan, S. P.; Knoot, P. A.; Benson, S. W. *Int. J. Chem. Kinet.* **1981**, *13*, 677−691.
(46) Seeley, J. V.; Jayne, J. T.; Molina, M. J. *J. Phys. Chem. A.* **1996**, *100*, 4019−4025.
(47) Takahashi, K.; Yamamoto, O.; Inomata, T. *Proc. Combust. Inst.* **2002**, *29*, 2447−2453.
(48) Bryukov, M. G.; Slagle, I. R.; Knyazev, V. D. *J. Phys. Chem. A* **2002**, *106*, 10532−10542.
(49) Corchado, J. C.; Truhlar, D. G.; Espinosa-Garcia, J. *J. Chem. Phys.* **2000**, *112*, 9375−9389.
(50) Rangel, C.; Navarrete, M.; Corchado, J. C.; Espinosa-García, J. *J. Chem. Phys.* **2006**, *124*, 124306 (124301−124319).
(51) Yang, M.-Y.; Yang, C.-L.; Chen, J.-Z.; Zhang, Q.-G. *Chem. Phys.* **2008**, *354*, 180−185.
(52) Miller, W. H. *Acc. Chem. Res.* **1976**, *9*, 306−312.
(53) Liu, Y.-P.; Lu, D.-H.; Gonzalez-Lafont, A.; Truhlar, D. G.; Garrett, B. C. *J. Am. Chem. Soc.* **1993**, *115*, 7806−7817.
(54) Roberto-Neto, O.; Coitino, E. L.; Truhlar, D. G. *J. Phys. Chem. A* **1998**, *102*, 4568−4578.
(55) Banks, S. T.; Clary, D. C. *Phys. Chem. Chem. Phys.* **2007**, *9*, 933−943.
(56) Yang, M.-y.; Yang, C.-L. *J. Mol. Struct. THEOCHEM* **2010**, *945*, 23−26.
(57) Feilberg, K. L.; Griffith, D. W. T.; Johnson, M. S.; Nielsen, C. J. *Int. J. Chem. Kinet.* **2005**, *37*, 110−118.
(58) Sellevåg, S. R.; Nyman, G.; Nielsen, C. J. *J. Phys. Chem. A* **2006**, *110*, 141−152.
(59) *NIST Standard Reference Database 144*, Online 1999 ed.; National Institute of Standards and Technology: Gaithersburg, MD, 2010, http://webbook.nist.gov/chemistry/.
(60) Wallington, T. J.; Hurley, M. D. *Chem. Phys. Lett.* **1992**, *189*, 437−442.
(61) Saueressig, G.; Bergamaschi, P.; Crowley, J. N.; Fischer, H.; Harris, G. W. *Geophys. Res. Lett.* **1996**, *23*, 3619−3622.
(62) Burkholder, J. B. Personal communication.
(63) Sauer, F.; Bauerle, S.; Burkholder, J. B.; Ravishankara, A. R. Temperature dependence of the Cl atom reaction with deuterated methanes. In *Faraday Discussion 130 Atmospheric Chemistry*; Royal Society of Chemistry and University of Leeds: Leeds, U.K, 2005.
(64) Russell, J. J.; Seetula, J. A.; Senkan, S. S.; Gutman, D. *Int. J. Chem. Kinet.* **1988**, *20*, 759−773.
(65) Eskola, A. J.; Seetula, J. A.; Timonen, R. S. *Chem. Phys.* **2006**, *331*, 26−34.
(66) Boone, G. D.; Agyin, F.; Robichaud, D. J.; Tao, F.-M.; Hewitt, S. A. *J. Phys. Chem. A* **2001**, *105*, 1456−1464.
(67) Chiltz, G.; Eckling, R.; Goldfinger, P.; Huybrechts, G.; Johnston, H. S.; Meyers, L.; Verbeke, G. *J. Chem. Phys.* **1963**, *38*, 1053−1061.
(68) Clyne, M. A. A.; Walker, R. F. *J. Chem. Soc., Faraday Trans. 1* **1973**, *69*, 1547−1567.
(69) Saueressig, G.; Bergamaschi, P.; Crowley, J. N.; Fischer, H.; Harris, G. W. *Geophys. Res. Lett.* **1995**, *22*, 1225−1228.
(70) Crowley, J. N.; Saueressig, G.; Bergamaschi, P.; Fischer, H.; Harris, G. W. *Chem. Phys. Lett.* **1999**, *303*, 268−274.
(71) Tyler, S. C.; Ajie, H. O.; Rice, A. L.; Cicerone, R. *J. Geophys. Res. Lett.* **2000**, *27*, 1715−1718.